

## Experimental mini-review on inclusive $V_{ub}$

---

Robert Kowalewski<sup>\*†</sup>

*University of Victoria, Canada*

*E-mail:* kowalews@uvic.ca

The current status of inclusive  $|V_{ub}|$  determinations is presented, along with a new  $|V_{ub}|$  determination from the BaBar collaboration based on the inclusive electron momentum spectrum. The importance of accounting for the dependence of measured partial branching fractions on the modeling of the  $\bar{B} \rightarrow X_u e \bar{\nu}$  decay is emphasized. Measurements and methods for use at future experiments are briefly discussed.

PoS (CKM2016) 040

*9th International Workshop on the CKM Unitarity Triangle*

*28 November - 3 December 2016*

*Tata Institute for Fundamental Research (TIFR), Mumbai, India*

---

<sup>\*</sup>Speaker.

<sup>†</sup>representing the BaBar collaboration.

## 1. Introduction and current status

The precise determination of  $|V_{ub}|$  is of high interest in understanding the physics of the quark flavor sector, which provides a unique window on CP violation and on particles at mass scales well beyond the reach of the highest energy accelerators. Semileptonic  $B$  decays allow relatively clean measurements, and theoretical tools enable decay rate calculations with uncertainties that can be meaningfully estimated. The total inclusive semileptonic decay rate to charmless final states,  $\Gamma(\bar{B} \rightarrow X_u e \bar{\nu})$  can be reliably calculated using an operator product expansion known as the Heavy Quark Expansion (HQE). Measuring this fully inclusive rate, however, presents a daunting challenge due to abundant semileptonic decays to charmed final states,  $\bar{B} \rightarrow X_c e \bar{\nu}$ . This large ( $\times 50$ ) background is suppressed kinematically using the charged lepton momentum,  $p_\ell$ , the invariant mass of the accompanying hadron,  $m_X$ , the  $q^2$  of the  $\ell \bar{\nu}$  system, the light-cone variable  $P_+ = E_X - |\vec{p}_X|$ , or some combination of these. While  $p_\ell$  can be determined by selecting charged leptons, the other quantities require reconstruction of all visible  $\Upsilon(4S)$  decay products, which reduces the yield by a factor of several hundred. Placing kinematic restrictions on the decays make calculations sensitive to the non-perturbative shape functions that describe the  $b$  quark distribution in the  $B$  meson. The clean region for theory is difficult for experiment and vice-versa.

All decay rate calculations are based on the HQE, but authors use different prescriptions for the treatment of the shape function and the renormalization scheme. An early approach (DN[1]) used  $\mathcal{O}(\alpha_s)$  corrections to the triple-differential decay distribution in leading-order HQE and a convolution of the parton-level spectrum with a parameterized shape function. This model is the basis for the simulations of inclusive semileptonic  $B$  decays that BaBar and Belle have used in their measurements of partial rates. It has been superceded by a calculation (BLNP[2]) that incorporates higher-order perturbative and power corrections in the shape-function mass renormalization scheme, and introduces additional shape functions at sub-leading orders. Another approach (GGOU[3]) based on the known higher-order corrections uses the kinetic mass renormalization scheme and absorbs all sub-leading shape functions into one of three  $q^2$ -dependent shape functions. A third approach (DGE[4]), in the  $\overline{MS}$  renormalization scheme, uses an NNLO resummation of soft gluons to calculate the shape function.

Experiments have measured partial decay rates for inclusive  $\bar{B} \rightarrow X_u e \bar{\nu}$  transitions in a variety of kinematic regions. These measurements, along with the decay rate calculations introduced above, result in the  $|V_{ub}|$  values given in Table 1. The results from the three calculations are consistent within the stated theoretical uncertainties, as are results from the different kinematic regions. The single largest (and correlated) parametric uncertainty on the average is from the  $b$  quark mass, which contributes  $\sim 2\%$ . Other sources of common systematic uncertainty come from still higher-order corrections to the rate, from the shape function(s), and from the experimental treatment of hadronization and the modeling of semileptonic  $B$  decays.

The  $|V_{ub}|$  values obtained from inclusive semileptonic decays are significantly higher than those determined in the exclusive decay  $\bar{B} \rightarrow \pi \ell \bar{\nu}$  (see Ref. [5]). This latter decay is cleaner experimentally and relies on a different set of theoretical tools (Lattice QCD). A gap of  $2\text{-}3\sigma$  between the inclusive and exclusive results has persisted for years. Recently, the determination of  $|V_{ub}|/|V_{cb}|$  from  $\Lambda_b$  semileptonic decays [12] also points to a smaller value for  $|V_{ub}|$ . The resolution of this inclusive-exclusive difference is a high priority for heavy flavour physics.

**Table 1:** Determinations of  $|V_{ub}|$  and their average. The first error is experimental, the second is from theoretical and parameteric uncertainties (from Ref. [5]).

Ref.	cut (GeV)	BLNP	GGOU	DGE
[6]	$E_e > 2.1$	$428 \pm 50^{+31}_{-36}$	$421 \pm 49^{+23}_{-33}$	$390 \pm 45^{+26}_{-28}$
[7]	$E_e - q^2$	$453 \pm 22^{+33}_{-38}$	not available	$417 \pm 20^{+28}_{-29}$
[8]	$E_e > 2.0$	$454 \pm 26^{+27}_{-33}$	$450 \pm 26^{+18}_{-25}$	$434 \pm 25^{+23}_{-25}$
[9]	$E_e > 1.9$	$493 \pm 46^{+27}_{-29}$	$493 \pm 46^{+17}_{-22}$	$485 \pm 45^{+21}_{-25}$
[10]	$\frac{q^2 > 8}{m_X < 1.7}$	$430 \pm 23^{+26}_{-28}$	$432 \pm 23^{+27}_{-30}$	$427 \pm 22^{+20}_{-20}$
[10]	$P_+ < 0.66$	$415 \pm 25^{+28}_{-27}$	$424 \pm 26^{+32}_{-32}$	$424 \pm 26^{+37}_{-32}$
[10]	$m_X < 1.55$	$430 \pm 20^{+28}_{-27}$	$429 \pm 20^{+21}_{-22}$	$453 \pm 21^{+24}_{-22}$
[10]	$E_\ell > 1$	$432 \pm 24^{+19}_{-21}$	$442 \pm 24^{+9}_{-11}$	$446 \pm 24^{+13}_{-13}$
[11]	$E_\ell > 1$	$449 \pm 27^{+20}_{-22}$	$460 \pm 27^{+10}_{-11}$	$463 \pm 28^{+13}_{-13}$
HFAG average		$445 \pm 16^{+21}_{-22}$	$451 \pm 16^{+12}_{-15}$	$452 \pm 16^{+15}_{-16}$

## 2. New BaBar result

The measurements in Table 1 were all published by 2012. A new measurement from BaBar has recently been submitted for publication[13]. The analysis uses the full BaBar dataset - 467M  $e^+e^- \rightarrow \Upsilon(4S) \rightarrow B\bar{B}$  events and an additional  $44.4\text{fb}^{-1}$  collected below  $B\bar{B}$  threshold. Events with electrons satisfying  $E_e > 0.8\text{ GeV}$  in the  $\Upsilon(4S)$  frame are selected, and a simple neural network is used to suppress the contribution from  $q\bar{q}$  ( $q = d, u, s, c$ ) continuum annihilations. The electron momentum spectrum, in bins of  $50\text{MeV}$ , is fitted to a sum of contributions. The continuum contribution is described by a 6-parameter empirical function, and the spectrum from  $\Upsilon(4S)$  decays is modeled as the sum of distinct contributions from several  $\bar{B} \rightarrow X_c e\bar{v}$  decay modes (specified below), from secondary electrons (primarily  $b \rightarrow c(\bar{c}) \rightarrow e^\pm$ ) and from signal  $\bar{B} \rightarrow X_u e\bar{v}$  decays. The models are built from decays generated with the EvtGen [14] and JETSET [15] programs and put through detailed simulation and reconstruction steps. The region near the endpoint of the electron momentum spectrum is highly sensitive to the modeling of the shape function; to reduce this sensitivity, all events with  $2.1 < E_e < 2.7\text{ GeV}$  are placed in one “wide bin” when performing the fit described below.

The components used to describe the  $\bar{B} \rightarrow X_c e\bar{v}$  spectrum are  $\bar{B} \rightarrow D e\bar{v}$ ,  $\bar{B} \rightarrow D^* e\bar{v}$ ,  $\bar{B} \rightarrow D^{(*)}\pi e\bar{v}$ ,  $\bar{B} \rightarrow D^{**} e\bar{v}$  and  $\bar{B} \rightarrow D'^{(*)} e\bar{v}$ ; the last of these corresponds to the radial excitations of the  $D$  and  $D^*$  mesons. The signal  $\bar{B} \rightarrow X_u e\bar{v}$  inclusive decays are initially generated using the DN model, and decays to resonant final states ( $X_R e\bar{v}$  where  $X_R = \pi, \eta, \rho, \eta', \omega$ ) are mixed in to preserve, as much as possible, the model distribution in  $q^2$ - $E_e$ - $m_X$  space. The  $E_e$  distribution is reweighted to represent the other (BLNP, GGOU, DGE) models. The parameteric input used in the model calculations is described fully in Ref. [13]; the values used for  $m_b$  and  $\mu_\pi^2$  come from Ref. [16].

A simultaneous fit to the spectra from the  $\Upsilon(4S)$  and below-resonance samples determines the parameters of the continuum function and the normalizations of the  $B$  decay components. The fit imposes two additional Gaussian constraints, on the ratio of the on/off-resonance  $q\bar{q}$  data sam-

ples and on the measured branching fraction for  $\bar{B} \rightarrow D e \bar{v}$ . The fit is performed for each of the aforementioned models and for different choices of parametric input. Systematic uncertainties are evaluated for experimental effects (backgrounds, efficiencies...), for parametric uncertainties ( $m_b$ ,  $\mu_\pi^2$ ,  $\alpha_s$ ) and for theoretical uncertainties.

Results for a representative set of input choices are listed in Table 2. The corresponding spectra, after subtraction of the continuum and  $B$  backgrounds based on the fit, are shown in Figure 1. The results supersede the previous BaBar electron spectrum measurement [8], and give  $|V_{ub}|$  values that are below the inclusive averages shown in Table 1.

Figure 1d shows the four model spectra on the same plot; this makes it clear that the normalization of the  $\bar{B} \rightarrow X_u e \bar{v}$  component is largely determined by the rate in the wide bin, where the signal to background is largest. The shape of the signal spectrum assumed in the fit has a significant impact on the determination of the partial branching fraction, in particular when the fit includes regions dominated by  $\bar{B} \rightarrow X_c e \bar{v}$  background. In this analysis, the same  $\bar{B} \rightarrow X_u e \bar{v}$  model was used to determine a partial branching fraction and to extract the corresponding  $|V_{ub}|$  value. This is in contrast to the  $|V_{ub}|$  values listed in Table 1, where all  $|V_{ub}|$  values for a given measurement are recalculated based on a published partial branching fraction that was determined using a single model (typically DN).

The new BaBar analysis illustrates the importance of model dependence in measured partial rates that include regions dominated by background from  $\bar{B} \rightarrow X_c e \bar{v}$  decays. This issue is likely to affect other measurements, in particular those that claim to measure the  $\bar{B} \rightarrow X_u e \bar{v}$  partial rate for  $E_\ell > 1$  GeV, which currently dominate the averages quoted in Table 1.

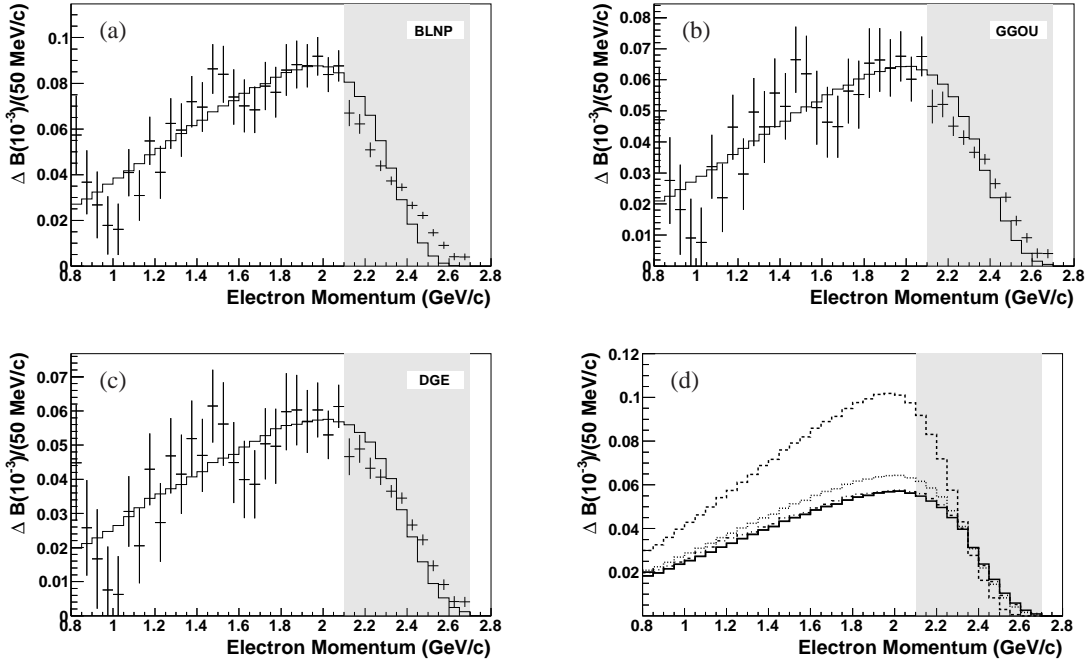
**Table 2:** Results for the partial branching fraction ( $\Delta\text{BF}$ ) and  $|V_{ub}|$  from fits to the inclusive electron spectrum in BaBar [13]. The two uncertainties on  $\Delta\text{BF}$  are experimental and theoretical, respectively. The errors listed on  $|V_{ub}|$  are due to experiment (first), theory (last), and the shape function (second of three, where present).

model	$\Delta\text{BF} \times 10^3$		$ V_{ub}  \times 10^3$	
	$E_e > 0.8$ (GeV)	$E_e > 2.1$ (GeV)	$E_e > 0.8$ (GeV)	$E_e > 2.1$ (GeV)
DN	$1.40 \pm 0.08^{+0.21}_{-0.15}$	$0.33 \pm 0.02^{+0.01}_{-0.01}$	$3.79 \pm 0.11^{+0.29}_{-0.22} {}^{+0.08}_{-0.07}$	$3.76 \pm 0.10^{+0.29}_{-0.22} {}^{+0.17}_{-0.15}$
DGE	$1.43 \pm 0.08$	$0.33 \pm 0.02$	$3.85 \pm 0.11 {}^{+0.08}_{-0.07}$	$3.82 \pm 0.10 {}^{+0.18}_{-0.16}$
GGOU	$1.55 \pm 0.08^{+0.10}_{-0.09}$	$0.34 \pm 0.02^{+0.01}_{-0.01}$	$3.96 \pm 0.10^{+0.16}_{-0.15} {}^{+0.04}_{-0.08}$	$3.92 \pm 0.10^{+0.16}_{-0.15} {}^{+0.17}_{-0.25}$
BLNP	$2.27 \pm 0.13^{+0.19}_{-0.16}$	$0.40 \pm 0.02^{+0.01}_{-0.01}$	$4.56 \pm 0.13^{+0.23}_{-0.21} {}^{+0.16}_{-0.16}$	$4.51 \pm 0.12^{+0.23}_{-0.20} {}^{+0.34}_{-0.28}$

### 3. Discussion

As demonstrated in the recent BaBar analysis, the determination of partial branching fractions for  $\bar{B} \rightarrow X_u e \bar{v}$  has model dependence that can be significant when including regions of phase space dominated by  $\bar{B} \rightarrow X_c e \bar{v}$ . The extent to which published measurements are affected by this is hard to estimate; *future measurements should account for this model dependence when determining  $|V_{ub}|$ .* Measuring the signal rate in background-dominated regions is fraught with difficulty. A more promising approach is to embrace the shape function dependence, using the precise spectra that can be obtained in the regions where  $\bar{B} \rightarrow X_c e \bar{v}$  decays are suppressed, to perform a global fit to these spectra (and those from  $b \rightarrow s \gamma$ ), thereby constraining the shape function as much as possible with experimental data. This approach is being pursued by independent groups [17, 18].

**Figure 1:** BaBar electron momentum spectra [13] (points) and calculated shape (histogram) for  $\bar{B} \rightarrow X_u e \bar{v}$  in the  $\Upsilon(4S)$  rest frame after subtracting backgrounds, for the (a) BLNP, (b) GGOU and (c) DGE models. The fit uses electrons in the range  $0.8 < E_e < 2.7$  GeV and combines all entries in the region  $2.1 < E_e < 2.7$  GeV into one bin. Panel (d) shows a comparison of the model spectra with normalization determined by the fits; from highest to lowest, the dashed curve is for BLNP, the dotted curve for GGOU, and the solid and dash-dotted curves, which overlap, for DN and DGE, respectively.



Additional supporting measurements will be valuable to better characterize the impact of weak annihilation,  $s\bar{s}$  production in hadronization, the modeling of exclusive states in  $\bar{B} \rightarrow X_u e \bar{v}$  and backgrounds from  $\bar{B} \rightarrow X_c e \bar{v}$  decays. For a discussion of these issues see Ref. [19].

## References

- [1] F. De Fazio and M. Neubert, JHEP **9906**, 017(1999).
- [2] B.O. Lange, M. Neubert, and G. Paz, Phys. Rev. D **72**, 073006(2005).
- [3] P. Gambino et al., JHEP **0710**, 058(2007).
- [4] J.R. Andersen and E. Gardi, JHEP **0601**, 097(2006).
- [5] Semileptonic bottom hadron decays and the determination of  $|V_{cb}|$  and  $|V_{ub}|$ , in C. Patrignani et al. (Particle Data Group), Chin. Phys. **C40**, 100001(2016).
- [6] A. Bornheim et al. (CLEO Collab.), Phys. Rev. Lett. **88**, 231803(2002).
- [7] B. Aubert et al. (BABAR Collab.), Phys. Rev. Lett. **95**, 111801(2005), Err.-*ibid.* **97**, 019903(E)(2006).
- [8] B. Aubert et al. (BABAR Collab.), Phys. Rev. D **73**, 012006(2006).
- [9] A. Limosani et al. (Belle Collab.), Phys. Lett. B **621**, 28(2005).

- [10] J. P. Lees et al. (BABAR Collab.), Phys. Rev. D**86**,032004(2012).
- [11] P. Urquijo et al. (Belle Collab.), Phys. Rev. Lett.**104**,021801(2010).
- [12] The LHCb collaboration, Nature Physics **11**, 743 (2015).
- [13] J. P. Lees et al. (BABAR Collab.), arXiv:1611.05624 [hep-ex].
- [14] D. J. Lange, Nucl. Instrum. Meth. A**462**,152(2001).
- [15] T. Sjöstrand, Comput. Phys. Commun. **82**,74(1994).
- [16] Heavy Flavor Averaging Group, Y. Amhis et al., arXiv:1412.7515v1 [hep-ex].
- [17] F. U. Bernlochner et al., arXiv:1011.5838 [hep-ph].
- [18] P. Gambino, K. J. Healy and C. Mondino, Phys. Rev. D**94**,014031(2016).
- [19] P. Urquijo talk at “Challenges in Semileptonic B decays,” MITP, Mainz,  
<https://tinyurl.com/hj4njbq>.